

Numerical analysis of high frequency electromagnetic field distribution and specific absorption rate in realistic breast models

Abstract. The knowledge of the electric field distribution in a female body plays a very important role in breast cancer detection. The aim of this paper is to present the numerical analysis of electric field distribution and SAR using the FDTD method in four kinds of realistic breast models. Three types of breast cancer have been used to demonstrate pathologies.

Streszczenie. Wiedza o rozkładzie pola elektrycznego w ciele kobiety ma wielkie znaczenie w detekcji raka. Praca niniejsza ma na celu przedstawienie numerycznej analizy rozkładu pola elektrycznego i SAR za pomocą metody FDTD w naturalistycznych czterech rodzajach piersi. Jako patologie zastosowano trzy rodzaje nowotworów piersi. (Numeryczna analiza rozkładu pola elektrycznego i SAR w naturalistycznym modelu piersi dla wysokich częstotliwości).

Keywords: Electric field distribution (E), SAR (Specific Absorption Rate), breast phantom, cancer
Słowa kluczowe: rozkład pola elektrycznego, współczynnik absorpcji, model piersi, nowotwór.

Introduction

The development of microwave breast cancer detection techniques, which has been seen in the last ten years, uses electromagnetic field (EMF) analysis in the context of electromagnetic hazards. According to the standard proposed by the Commission on Non-Ionizing Radiation Protection – ICNIRP [2] and adopted by EU as the norm, parameters which are required for estimation of EMF exposures in the frequency ranging from 10 MHz to 10 GHz comprise electric field (E) and Specific Absorption Rate (SAR).

The SAR value is defined in the official 2008/46/WE directive [2,6] of the European Parliament and Council, a document prepared on the basis of ICNIRP report. In most countries, these guidelines have been adopted as the basic limits on SAR, to avoid adverse health effects related to whole-body heat stress and excessive localized tissue heating for frequencies between 3 kHz and 300 GHz.

Numerical analysis

In order to estimate the electric field and SAR distribution in the female breast the authors have used freely available database of breast models [10]. These breast phantoms derive from series of T1-weighted magnetic resonance images (MRIs). The numerical phantoms are classified according to their radiographic density, defined by the American College of Radiology. The models are divided into four categories: class 1 - mostly fatty (<25% glandular tissues), class 2 - scattered fibroglandular (25-50% glandular tissue), class 3 - heterogeneously dense (50-75% glandular tissue) and class 4 - extremely dense (>75% glandular tissue) [9,10].

In our study the electrical properties of the breast models are calculated for frequencies of 2.45 GHz and 6GHz with regard to Debye'a equation [1] with parameters taken from Lazebnik [3].

Table 1. Debye'a parameters of tissues used during numerical analysis [8]

Tissue	ϵ_s	ϵ_∞	$\Delta\epsilon$	σ_s [S/m]
Adipose	2.42-7.63	2.28-4.09	0.14-3.52	0.002-0.08
Transitional	7.63-36.7	4.09-16.8	3.54-19.9	0.084-0.46
Fibroglandular	36.7-67.2	16.8-29.1	19.9-38.1	0.461-1.38
Skin	40.1	15.3	24.8	0.74

$$(1) \underline{\epsilon}(\omega) = \epsilon'(\omega) - j\epsilon''(\omega) = \epsilon_\infty + \frac{\Delta\epsilon}{1 + j\omega\tau} + \frac{\sigma_s}{j\omega\epsilon_0}$$

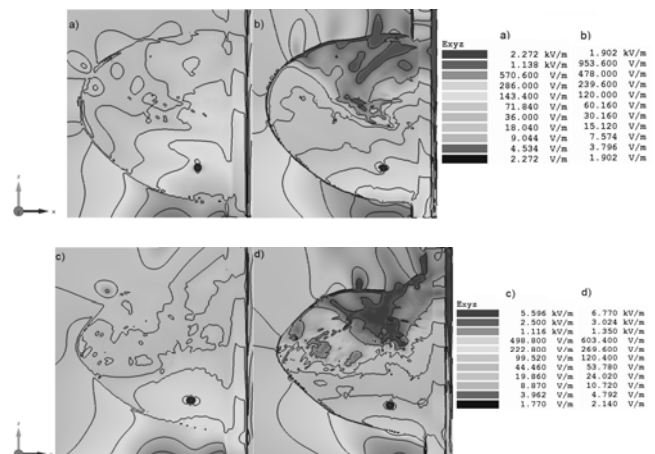
where: ω – angular frequency, $\Delta\epsilon = \epsilon_\infty - \epsilon_s$ – dielectric increment, ϵ_s – electric permittivity, ϵ_0 – permittivity of vacuum, σ_s – static conductivity, τ - relaxation time

Table 2. Debye'a parameters of malignant tissues used during numerical analysis [8]

Tissue	ϵ_s	ϵ_∞	$\Delta\epsilon$	σ_s [S/m]
Endogenous	56.6	18.8	37.8	0.803
Bubbles	39.7	13.2	26.5	0.562
Nanotubes	63.3	14.8	54.5	1.47

To excite the electromagnetic field, a dipole antenna was used. The dipole was prepared for two resonance frequencies: $f_c = 2.45$ GHz and $f_c = 6$ GHz.

The diameter of the inclusion in the breast interior varies from 2mm, 6mm, 10mm to 22mm. The dielectric parameters of each malignant tumor was calculated according to the values presented in Table 2 for endogenous, bubbles and nanotubes cancerous tissues. The examples of electric field distribution can be seen in Figure1.



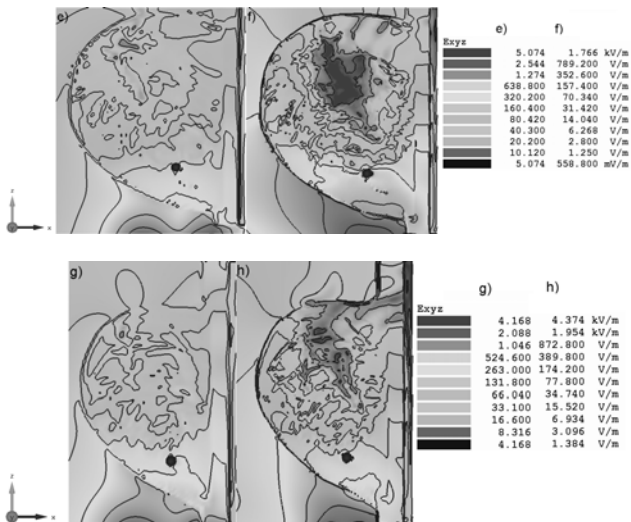


Fig.1. Electric field distribution in realistic breast models: a) class 1 for 2,45GHz, b) class 1 for 6GHz, c) class 2 for 2,45GHz, d) class 2 for 6GHz, e) class 3 for 2,45GHz, f) class 3 for 6GHz, g) class 4 for 2,45GHz, h) class 4 for 6GHz.

A survey of the size of tumours detected in a large collection of breast cancer studies of various modalities shows that the median diameter of the detected tumour ranges from 10 to 20mm [7]. The occurrence of cancer is prevalent in axillary lymph nodes.

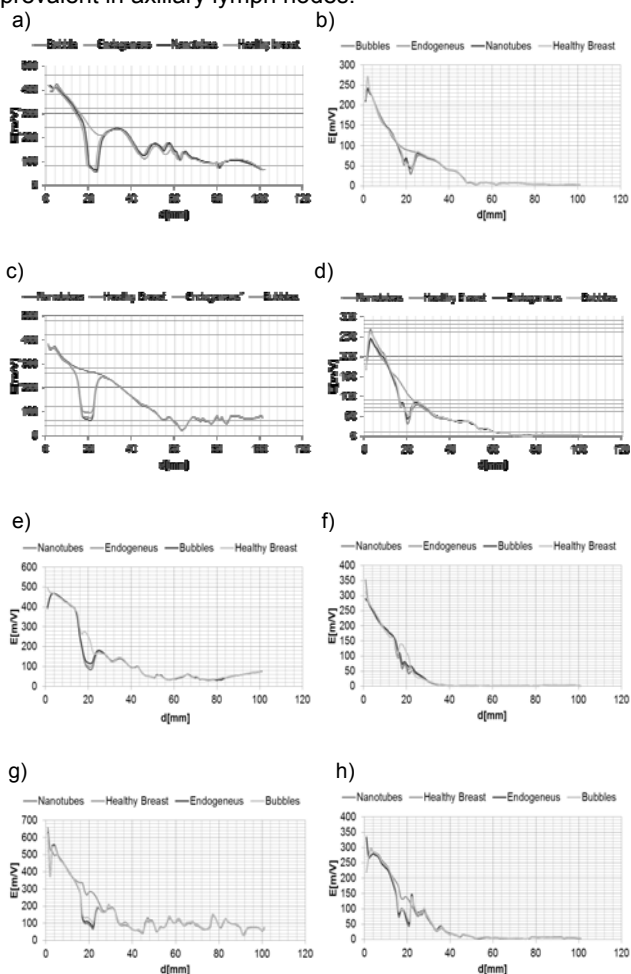


Fig.2. Electric field distribution along the x-axis for 6 mm diameter cancer in realistic breast models: a) class 1 for 2,45GHz, b) class 1 for 6GHz, c) class 2 for 2,45GHz, d) class 2 for 6GHz, e) class 3 for 2,45GHz, f) class 3 for 6GHz, g) class 4 for 2,45GHz, h) class 4 for 6GHz.

In our models we used one transmitter-receiver dipole antenna. After the transmission of a signal, its reflection is received by the same antenna. The comparison of signals for the pathological and healthy breast shows that the signals are different. From the obtained distributions of the electric field and its characteristics it can be seen that the distributions are heterogeneous.

SAR

SAR is a measure of the rate at which energy is absorbed by the body when exposed to a high frequency electromagnetic field. It is defined as the power absorbed per mass of tissue and has units of watts per kilogram (W/kg). SAR is usually averaged either over the whole body, or over a small sample volume (typically 1 g or 10 g of tissue).

SAR can be calculated from the electric field within the tissue as [4,5,6]:

$$(2) \quad SAR = \frac{\sigma |E|^2}{\rho}$$

where: σ - conductivity of tissue [S/m], ρ - density of the tissue [kg/m^3], E - electric field in the tissue.

The exemplary distributions of SAR for 6mm cancer can be seen in Figure 3.

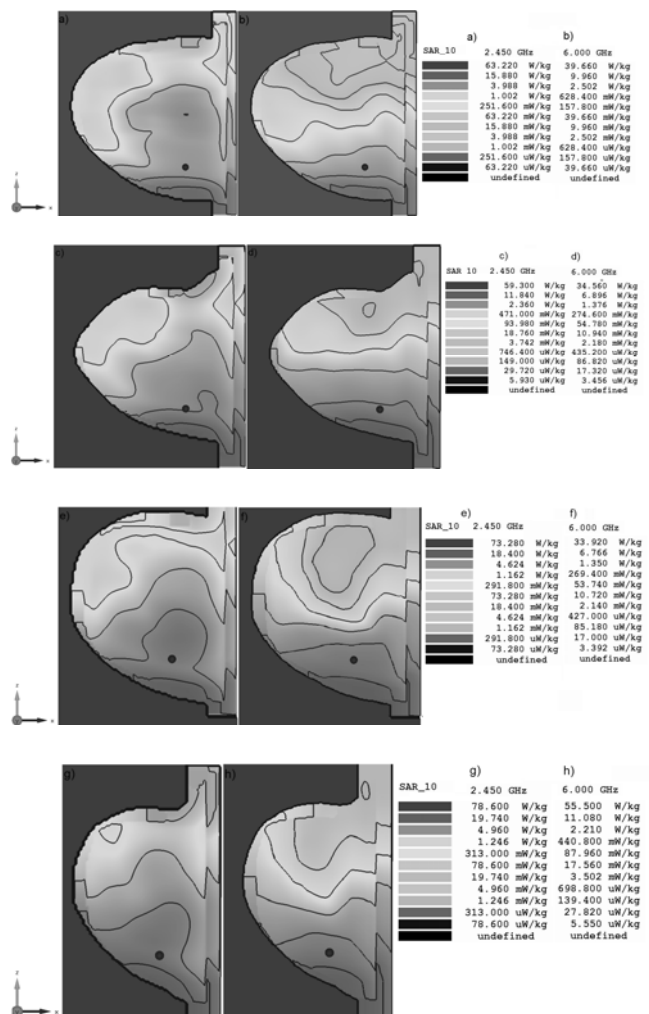


Fig.3. SAR_{10g} distribution 6 mm diameter endogenous cancer in realistic breast models: a) class 1 for 2,45GHz, b) class 1 for 6GHz, c) class 2 for 2,45GHz, d) class 2 for 6GHz, e) class 3 for 2,45GHz, f) class 3 for 6GHz, g) class 4 for 2,45GHz, h) class 4 for 6GHz.

In the obtained images of the SAR_{10g} distribution it can be seen that the distributions are heterogeneous.

Conclusions

On the basis of the simulation the authors have received the electric field distribution and SAR in the analysed models. Comparing the distribution of the electric field along the x-axis of the healthy breast with the pathological one it can be seen where a tumor occurs. The analysis of the distribution of the electric field for 2.45GHz and 6 GHz, shows that 2.45GHz values of electric fields are larger than 6GHz.

REFERENCES

- [1] Gabriel C. „The dielectric properties of biological tissue: I. Literature survey, *Phys. Med. Biol.*, vol.41(1996), pp.2231-2249,
- [2] http://rop.sejm.gov.pl/1_Old/opracowania/pdf/material30.pdf,
- [3] Lazebnik M, and all, A large-scale study of ultrawideband microwave dielectric properties of normal, benign, and malignant breast tissues obtained from cancer surgeries, *Phys. Med. Biol.* 52 6093-115 (2007),
- [4] Miaskowski A., Wac-Włodarczyk A., Olchowiak G., Low frequency FDTD Algorithm and its Application to Inductive Hyperthermia, *Przegląd Elektrotechniczny*, ISSN 0033-2097, R. 88 NR 6/2012,
- [5] Miaskowski A. „ Zastosowanie mikrofal do detekcji raka sutka”, *Przegląd Elektrotechniczny* pp.87-88, 12/2005,
- [6] Miaskowski A., Krawczyk A., Wac-Włodarczyk A., „Zastosowanie promieniowania mikrofalowego w detekcji raka gruczołu piersiowego” Warszawa ,*CIOP-PIB* 2007,

- [7] Michaelson J S, and all, Gauging the impact of breast carcinoma screening in terms of tumor size and death rate, *Cancer* 982114-24, (2003).
- [8] Shea J.D., and all , Contrast-enhanced microwave imaging of breast tumors: a computational study using 3D realistic numerical phantoms, *Inverse Problems*, vol. 26(2010), 22pp,
- [9] Shea D.J., Kosmas P., Hagness C.S., Van Veen B.D, “ Three-dimensional microwave imaging of realistic numerical breast phantoms via a multiple-frequency inverse scattering technique”, *Med. Phys.* 37 (8), August 2010,
- [10] Zastrow E., at all, Database of 3D Grid-Based Numerical Breast Phantoms for use in Computational Electromagnetics Simulations, University of Wisconsin, <http://uwcem.ece.wisc.edu/home.htm>,

Authors: mgr inż. Joanna Michałowska-Samonek, *Politechnika Lubelska, Instytut Podstaw Elektrotechniki i Elektrotechnologii, ul.Nadbystrzycka38a, 20-618 Lublin, Email: joannamichalowska@o2.pl, Dr.hab inż., Prof.PL, Andrzej Wac-Włodarczyk, Politechnika Lubelska, Instytut Podstaw Elektrotechniki i Elektrotechnologii, E-mail: a.wac-wlodarczyk@pollub.pl, Dr inż. Arkadiusz Miaskowski, Katedra Zastosowań Matematyki i Informatyki, Uniwersytet Przyrodniczy w Lublinie, 20-950 Lublin, ul. Akademicka 13, E-mail: arek.miaskowski@up.lublin.pl.*